fractal and fractional

MDPI

Article

A Chebyshev Collocation Approach to Solve Fractional Fisher–Kolmogorov–Petrovskii–Piskunov Equation with Nonlocal Condition

Dapeng Zhou [1], Afshin Babaei [2], Seddigheh Banihashemi [2], Hossein Jafari [2,3,4,*], Jehad Alzabut [5,6] and Seithuti P. Moshokoa [7]

1 School of Mathematics and Quantitative Economics, Shandong University of Finance and Economics, Jinan 250014, China; dapengzhou225@outlook.com
2 Department of Applied Mathematics, University of Mazandaran, Babolsar 4741613534, Iran; babaei@umz.ac.ir (A.B.); s.banihashemi@stu.umz.ac.ir (S.B.)
3 Department of Mathematical Sciences, University of South Africa (UNISA), Pretoria 0003, South Africa
4 Department of Medical Research, China Medical University Hospital, China Medical University, Taichung 110122, Taiwan
5 Department of Mathematics and Sciences, Prince Sultan University, Riyadh 11586, Saudi Arabia; jalzabut@psu.edu.sa
6 Department of Industrial Engineering, OSTİM Technical University, Ankara 06374, Turkey
7 Department of Mathematics and Statistics, Tshwane University of Technology, Pretoria 0008, South Africa; moshokoasp@tut.ac.za
* Correspondence: jafari.usern@gmail.com

Abstract: We provide a detailed description of a numerical approach that makes use of the shifted Chebyshev polynomials of the sixth kind to approximate the solution of some fractional order differential equations. Specifically, we choose the fractional Fisher–Kolmogorov–Petrovskii–Piskunov equation (FFKPPE) to describe this method. We write our approximate solution in the product form, which consists of unknown coefficients and shifted Chebyshev polynomials. To compute the numerical values of coefficients, we use the initial and boundary conditions and the collocation technique to create a system of equations whose number matches the unknowns. We test the applicability and accuracy of this numerical approach using two examples.

Keywords: fractional Fisher–Kolmogorov–Petrovskii–Piskunov equation; collocation scheme; sixth-kind Chebyshev polynomials; convergence analysis

Citation: Zhou, D.; Babaei, A.; Banihashemi, S.; Jafari, H.; Alzabut, J.; Moshokoa, S.P. A Chebyshev Collocation Approach to Solve Fractional Fisher–Kolmogorov–Petrovskii–Piskunov Equation with Nonlocal Condition. *Fractal Fract.* **2022**, *6*, 160. https://doi.org/10.3390/fractalfract6030160

Academic Editor: Hijaz Ahmad

Received: 10 January 2022
Accepted: 10 February 2022
Published: 15 March 2022

1. Introduction

A study of generalized derivatives and integrals has gained considerable popularity in the last few years, mainly due to its attractive applications in numerous diverse fields such as fluid flow [1], finance [2] and physics [3]. These generalized derivatives and integrals are called fractional derivatives and integrals, respectively [4–6]. They are more flexible for real-world applications since they can have both integer and noninteger operators. Fractional derivatives are well-known for their utility in describing the memory and heredity features of a variety of materials and processes [7–10]. Nikan et al. [11] considered the fractional nonlinear sine-Gordon and Klein–Gordon models arising in relativistic quantum mechanics. Babaei et al. [12] introduced a class of time-fractional stochastic heat equations driven by Brownian motion. Numerical solution of time fractional convection–diffusion-wave equation based on RBF method is described in [13,14]. Zaky et al. [15] applied some pseudospectral methods for solving the Riesz space-fractional Schrödinger equation. Lately, countless researchers are contributing to new models based on fractional equations. Among which, the generalized Fisher–Kolmogorov–Petrovskii–Piskunov equation has substantial attention [16–19].

In this paper, we introduce the FFKPPE in the form

$$ {}_0\mathscr{D}_t^{\eta} u(x,t) = \mu \Delta u(x,t) + \beta \nabla u(x,t) + \frac{\kappa}{\zeta} \int_0^t e^{-\frac{t-s}{\zeta}} \Delta u(x,\mathrm{s}) \mathrm{ds} + \mathscr{F}(x,t,u), \tag{1} $$

where $(x,t) \in \Omega_{\mathrm{L}} \times \Omega_{\mathrm{T}}$, with the following initial and boundary conditions

$$ u(x,0) = u_0(x), \qquad x \in \Omega_{\mathrm{L}}, \tag{2} $$

$$ \mathrm{g}(u(0,t)) = \rho_0(t), \qquad t \in \Omega_{\mathrm{T}}, \tag{3} $$

$$ \hat{\theta} u(\mathrm{L},t) + \hat{\delta} u_x(\mathrm{L},t) = \rho_{\mathrm{L}}(t), \qquad t \in \Omega_{\mathrm{T}}, \tag{4} $$

where $\Delta := \frac{\partial^2}{\partial x^2}$ is the Laplace operator and $\nabla := \frac{\partial}{\partial x}$. Further, μ, β, κ, $\zeta \neq 0$, $\hat{\theta}$ and $\hat{\delta}$ are given real constants. Moreover, $\Omega_{\mathrm{L}} := [0, \mathrm{L}]$, $\Omega_{\mathrm{T}} := [0, \mathrm{T}]$, the nonlinear source term $\mathscr{F}(x,t,u) \in \mathbf{C}^1(\Omega_{\mathrm{L}} \times \Omega_{\mathrm{T}} \times \mathbb{R})$ fulfills the Lipschitz condition in terms of u and $u_0(x)$, $\rho_0(t)$ and $\rho_{\mathrm{L}}(t)$ are regarded as known continuous functions. In addition, the nonlinear function g of $u(0,t)$ is given and the operator ${}_0\mathscr{D}_t^{\eta}[\cdot]$ denotes the Caputo fractional derivative of order $\eta \in (0,1)$ defined as [20]:

$$ {}_0\mathscr{D}_t^{\eta} u(x,t) = \frac{1}{\Gamma(1-\eta)} \int_0^t (t-s)^{-\eta} u_s(x,s) \mathrm{ds}, \tag{5} $$

in which $\Gamma(\cdot)$ denotes the Gamma function. The generalized FFKPPE (1), belongs to the class of reaction–diffusion equations. It is commonly used to represent practical situations that often arise in physics, chemistry and biology [18,19,21]. A more specific example is in the modeling of genetic behavior in the growth of micro-organisms [22].

In the literature, the problem (1)–(4) has been considered analytically and numerically. For instance, Araújo et al. [23] investigated the stability of the model represented by (1), while also investigating the qualitative features of its solutions obtained under Dirichlet boundary conditions. Splitting methods were created for purposes of numerically studying the qualitative nature of the solutions. A list of numerical approaches has been proposed and studied for different cases of the Equation (1). Branco et al. [16] studied the approach of method of lines for the numerical solution to integro-differential equation of type (1). In their work, Araújo et al. [24] developed the famous Fisher equation by investigating the qualitative features of the numerical traveling wave solutions of integro-differential equations. The hyperbolic equation equivalence was used to replace the integro-differential equation, allowing for the numerical quantification of the velocity of traveling wave solutions. While studying the effects on memory factors in phenomena of diffusion [25] developed approximation methods for computing integro-differential equations. Barbeiro and Ferreira [26] provided mathematical models to describe medication absorption through the skin. The development of these models involved extending the traditional Fick's law by incorporating a memory term. This replaces the classical models of advection–diffusion equations with integro-differential equations. The well-posedness of model was investigated using Neumann, Dirichlet and natural boundary conditions. The methods for computing numerical solutions were proposed. In addition, their stability and convergence were studied, while including a presentation of numerical simulations to illustrate the behavior of the model. Khuri and Sayfy proposed a numerical scheme to solve a generalized Fisher integro-differential equation using finite differences and spline collocation in [17]. To manage the numerical integration, a composite weighted trapezoidal rule was used, resulting in a closed-form difference scheme. To assess the method's accuracy, multiple test examples were solved. The scheme's convergence and stability were also explored. Babaei et al. sets up a numerical technique that makes use of the Chebyshev polynomials of the sixth kind with the main purpose of approximating the solutions of integro-differential equations of variable order [27]. The sixth-kind Chebyshev polynomials are a special case of the general nonsymmetric class mentioned in [28,29].

We subdivide our research under different headings as follows. In the next section, we focus on fundamental mathematical concepts that lay important groundwork for the subsequent sections. Section 3 outlines the methodology that we use to conduct our research and in the fourth section we study the convergence of this methodology. In Section 5, we apply the methodology to specific examples. We mention our findings and give suggestions in the last section of this manuscript.

2. Preliminaries

For use in sequel, this section presents the basic properties of the sixth-kind Chebyshev polynomials and related necessary definitions.

Definition 1. *We define the Riemann–Liouville fractional integral with order $\eta \in (0,1)$ as [20]*

$$\mathrm{I}_t^{\eta} u(x,t) = \frac{1}{\Gamma(\eta)} \int_0^t u(x,s)(t-s)^{\eta-1} \mathrm{d}s.$$

Definition 2 ([12])**.** *The following recurrence relation is used to obtain the sixth-kind Chebyshev polynomials $\hat{\phi}_q(t)$*

$$\hat{\phi}_0(t) = 1, \quad \hat{\phi}_1(t) = t,$$
$$\hat{\phi}_{q+1}(t) = t\,\hat{\phi}_q(t) + \varrho_q \hat{\phi}_{q-1}(t), \quad q = 2,3,\ldots,$$

where

$$\varrho_q := \frac{-(q+1-(-1)^q)(q+2-(-1)^q)}{4(q+1)(q+2)}.$$

Definition 3 ([29])**.** *Considering the interval $[0,\mathrm{T}]$, then the shifted sixth-kind Chebyshev polynomials are written as*

$$\phi_q(t) = \hat{\phi}_q((2/\mathrm{T})t - 1), \quad q = 0,1,2,\ldots$$

In analytical format, these polynomials are presented as [29]

$$\phi_q(t) = \sum_{k=0}^{q} \mathscr{L}_{k,q} t^k, \tag{6}$$

where

$$\mathscr{L}_{k,q} = \begin{cases} \frac{2^{2k-q}}{(2k+1)!\,\mathrm{T}^k} \sum\limits_{p=\lfloor \frac{k+1}{2} \rfloor}^{\frac{q}{2}} \frac{(-1)^{\frac{q}{2}+p+k}(2p+k+1)!}{(2p-k)!}, & q \text{ even}, \\ \frac{2^{2k-q+1}}{(2k+1)!(q+1)\,\mathrm{T}^k} \sum\limits_{p=\lfloor \frac{k}{2} \rfloor}^{\frac{q-1}{2}} \frac{(-1)^{\frac{q+1}{2}+p+k}(p+1)(2p+k+2)!}{(2p-k+1)!}, & q \text{ odd}. \end{cases}$$

Let $\mathbf{L}^2_{\varpi}(\Omega_{\mathrm{L}} \times \Omega_{\mathrm{T}})$ represent a space that consists of square integrable functions having variables (x,t) and the weight function $\varpi(x,t) = w(x)w(t)$ with $w(x) = \sqrt{x-x^2}(2x-1)^2$.

Theorem 1. *We assume that $f(x,t) \in \mathbf{L}^2_{\varpi}(\Omega_{\mathrm{L}} \times \Omega_{\mathrm{T}})$ satisfies the expansion [12]*

$$f(x,t) = \sum_{p=0}^{\infty} \sum_{q=0}^{\infty} c_{p,q} \phi_p(x) \phi_q(t).$$

Suppose $\left\| \frac{\partial^6 f(x,t)}{\partial x^3 \partial t^3} \right\|_2 \leq \hat{c}$ and $\hat{c} > 0$. The inequality $|c_{p,q}| < \frac{\hat{c}}{p^3 q^3}$ for all $p,q > 3$, is satisfied for the expansion coefficients. Further, if

$$f(x,t) \simeq f_{n,m}(x,t) = \sum_{p=0}^{n} \sum_{q=0}^{m} c_{p,q} \phi_p(x) \phi_q(t), \tag{7}$$

is an estimate for $f(x,t)$*, then*

$$|f(x,t) - f_{n,m}(x,t)| < \frac{\hat{c}}{2^{n+m}},$$

$$\left|\nabla f(x,t) - \nabla f_{n,m}(x,t)\right| < \sigma \frac{n}{2^{n+m-2}},$$

$$\left|\Delta f(x,t) - \Delta f_{n,m}(x,t)\right| < \hat{\sigma} \frac{n^3}{2^{n+m-8}},$$

where $\sigma, \hat{\sigma} > 0$*.*

Definition 4. *Suppose* $\mathrm{P}_{p+1}(t)$ *is Legendre polynomial of order* $p+1$ *on* $[-1,1]$*. The Legendre–Gauss quadrature formula for* $g(t) \in \mathbf{C}[a,b]$ *is defines as:*

$$\int_a^b g(t)\mathrm{d}t = \frac{b-a}{2} \sum_{r=0}^{\mathrm{M}} \mathtt{w}_r \, g\Big(\frac{b-a}{2}\varsigma_r + \frac{b+a}{2}\Big),$$

in which distinct nodes $\{\varsigma_r\}_{r=0}^{\mathrm{M}}$ *are the zeros of* $\mathrm{P}_{\mathrm{M}+1}(t)$ *and* $\{\mathtt{w}_r\}_{r=0}^{\mathrm{M}}$ *are the corresponding weights [30]*

$$\mathtt{w}_r = \frac{2}{(1-\varsigma_r^2)(\mathrm{P}'_{\mathrm{M}+1}(\varsigma_r))^2}.$$

3. Numerical Method

In this section, we describe numerical technique for solving (1)–(4) on the basis of the shifted sixth-kind Chebyshev polynomials. We obtain the numerical approximation of Equation (1) by considering an approximation of the fractional derivative of the unknown function as:

$${}_0\mathscr{D}_t^{\eta} u(x,t) \simeq {}_0\mathscr{D}_t^{\eta} u_{n,m}(x,t) = \sum_{p=0}^{n}\sum_{q=0}^{m} c_{p,q}\phi_p(x)\phi_q(t) = \Phi(x)^{\mathrm{T}}\mathbf{C}\Phi(t), \tag{8}$$

in which

$$\Phi(x) = [\phi_0(x), \phi_1(x), \ldots, \phi_n(x)]^{\mathrm{T}}, \tag{9}$$

$$\Phi(t) = [\phi_0(t), \phi_1(t), \ldots, \phi_m(t)]^{\mathrm{T}}, \tag{10}$$

and

$$\mathbf{C} = \Big[c_{p,q}\Big]_{(n+1)\times(m+1)}, \qquad p = 0,\ldots,n, \;\; q = 0,\ldots,m,$$

represent a matrix with unknown entries whose numerical values are to be computed. According to Definition 1 and the initial condition (2)

$$u(x,t) \simeq \mathrm{I}_t^{\eta}\Big(\Phi(x)^{\mathrm{T}}\mathbf{C}\Phi(t)\Big) + u_0(x) = \Phi(x)^{\mathrm{T}}\mathbf{C}\,\mathrm{I}_t^{\eta}\Phi(t) + u_0(x).$$

By applying Definition 1 and shifted SKCPs (6), for $q = 0,\ldots,m$

$$\Lambda_q^{\eta}(t) := \mathrm{I}_t^{\eta}\phi_q(t) = \sum_{k=0}^{q} \mathscr{L}_{k,q}\mathrm{I}_t^{\eta}(t^k) = \sum_{k=0}^{q} \mathscr{L}_{k,q}^{\eta} t^{k+\eta},$$

where $\mathscr{L}_{k,q}^{\eta} := \mathscr{L}_{k,q}\frac{\Gamma(k+1)}{\Gamma(k+1+\eta)}$, thus, we let

$$u(x,t) \simeq u_{n,m}(x,t) = \Phi(x)^{\mathrm{T}}\mathbf{C}\Phi_t^{\eta}(t) + u_0(x), \tag{11}$$

such that

$$\Phi_t^{\eta}(t) := \left[\Lambda_0^{\eta}(t), \Lambda_1^{\eta}(t), \ldots, \Lambda_m^{\eta}(t)\right]^{\mathrm{T}}. \tag{12}$$

According to (1) and (11)

$$\begin{aligned}\mathbf{R}(x,t) := {} & \Phi(x)^{\mathrm{T}}\mathbf{C}\Phi(t) - \mu\Big(\Phi_{xx}(x)^{\mathrm{T}}\mathbf{C}\Phi_t^{\eta}(t) + u_0''(x)\Big) \\ & - \beta\Big(\Phi_x(x)^{\mathrm{T}}\mathbf{C}\Phi_t^{\eta}(t) + u_0'(x)\Big) \\ & - \frac{\kappa}{\zeta}\int_0^t e^{-\frac{t-s}{\zeta}}\Big(\Phi_{xx}(x)^{\mathrm{T}}\mathbf{C}\Phi_s^{\eta}(s) + u_0''(x)\Big)\mathrm{ds} \\ & - \mathscr{F}\Big(x,t,\Phi(x)^{\mathrm{T}}\mathbf{C}\Phi_t^{\eta}(t) + u_0(x)\Big),\end{aligned} \tag{13}$$

with

$$\Phi_x(x) = \left[\phi_0'(x), \phi_1'(x), \ldots, \phi_n'(x)\right]^{\mathrm{T}}, \tag{14}$$

$$\Phi_{xx}(x) = \left[\phi_0''(x), \phi_1''(x), \ldots, \phi_n''(x)\right]^{\mathrm{T}}. \tag{15}$$

In addition, from Equation (11) and the initial and boundary conditions (2)–(4), we define

$$\Psi(x) := \Phi(x)^{\mathrm{T}}\mathbf{C}\Phi_t^{\eta}(0) + u_0(x), \tag{16}$$

$$\Pi_1(t) := \mathrm{g}\Big(\Phi(0)^{\mathrm{T}}\mathbf{C}\Phi_t^{\eta}(t) + u_0(0)\Big) - \rho_0(t), \tag{17}$$

$$\begin{aligned}\Pi_2(t) := {} & \hat{\theta}\Big(\Phi(\mathtt{L})^{\mathrm{T}}\mathbf{C}\Phi_t^{\eta}(t) + u_0(\mathtt{L})\Big) \\ & + \hat{\delta}\Big(\Phi_x(\mathtt{L})^{\mathrm{T}}\mathbf{C}\Phi_t^{\eta}(t) + u_0'(\mathtt{L})\Big) - \rho_{\mathtt{L}}(t).\end{aligned} \tag{18}$$

Let $x_0 = 0, x_n = \mathtt{L}$. We denote the roots of $\phi_{n-1}(x)$ and $\phi_m(t)$ to be $\{x_p : p = 1, \ldots, n-1\}$ and $\{t_q : q = 1, \ldots, m\}$, respectively. If we evaluate (16)–(18) at the respective collocation points (x_p, t_q), $p = 1, \ldots, n-1$, and $q = 1, \ldots, m$, then

$$\begin{aligned}\mathbf{R}(x_p,t_q) = {} & \Phi(x_p)^{\mathrm{T}}\mathbf{C}\Phi(t_q) - \mu\Big(\Phi_{xx}(x_p)^{\mathrm{T}}\mathbf{C}\Phi_t^{\eta}(t_q) + u_0''(x_p)\Big) \\ & - \beta\Big(\Phi_x(x_p)^{\mathrm{T}}\mathbf{C}\Phi_t^{\eta}(t_q) + u_0'(x_p)\Big) \\ & - \frac{\kappa}{\zeta}\underbrace{\int_0^{t_q} e^{-\frac{t_q-s}{\zeta}}\Big(\Phi_{xx}(x_p)^{\mathrm{T}}\mathbf{C}\Phi_s^{\eta}(s) + u_0''(x_p)\Big)\mathrm{ds}}_{\mathscr{E}_{p,q}} \\ & - \mathscr{F}\Big(x_p,t_q,\Phi(x_p)^{\mathrm{T}}\mathbf{C}\Phi_t^{\eta}(t_q) + u_0(x_p)\Big).\end{aligned} \tag{19}$$

Due to Definition 4, $\mathscr{E}_{p,q}$ can be approximated as

$$\begin{aligned}\mathscr{E}_{p,q} &= \int_0^{t_q} e^{-\frac{t_q-s}{\zeta}}\Big(\Phi_{xx}(x_p)^{\mathrm{T}}\mathbf{C}\Phi_s^{\eta}(s) + u_0''(x_p)\Big)\mathrm{ds} \\ &= \frac{t_q}{2}\sum_{r=0}^{\mathrm{M}}\mathtt{w}_r\left(e^{-\frac{t_q-s_{r,q}}{\zeta}}\Big(\Phi_{xx}(x_p)^{\mathrm{T}}\mathbf{C}\Phi_t^{\eta}(s_{r,q}) + u_0''(x_p)\Big)\right),\end{aligned} \tag{20}$$

where $s_{r,q} = \frac{t_q}{2}\varsigma_r + \frac{t_q}{2}$. Thus, replacing (20) in (19) and considering (16)–(18) at the collocation points (x_p, t_q), yield

$$\mathbf{R}(x_p, t_q) = 0, \qquad p = 1, \ldots, n-1, \quad q = 1, \ldots, m, \tag{21}$$
$$\Pi_1(t_q) = 0, \qquad q = 1, \ldots, m, \tag{22}$$
$$\Pi_2(t_q) = 0, \qquad q = 1, \ldots, m, \tag{23}$$
$$\Psi(x_p) = 0, \qquad p = 0, \ldots, n. \tag{24}$$

The relations (21)–(24) imply that we deduce an $(n+1) \times (m+1)$ system of nonlinear equations that can be solved through a numerical approach, such as the Newton iteration technique, to achieve the numerical values of $c_{p,q}$, $p = 0, 1, \ldots, n$, $q = 0, \ldots, m$. The given method in this section is listed as Algorithm 1.

Algorithm 1: Algorithm of presented method in Section 3

Input: $\mathtt{L}, \mathtt{T}, \mu, \beta, \kappa, \zeta, \hat{\theta}, \hat{\delta}$ and $n, m, \mathtt{M} \in \mathbb{Z}^+$, $\eta \in (0,1)$ and functions F, g, u_0, ρ_0 and $\rho_{\mathtt{L}}$.
Step 1: Compute the shifted sixth-kind Chebyshev polynomials $\phi_i(x)$ on the interval $[0, \mathtt{L}]$ and $\phi_j(t)$ on the interval $[0, \mathtt{T}]$.
Step 2: Compute the vector of shifted sixth-kind Chebyshev polynomials $\Phi(x)$ and $\Phi(t)$ from Equations (9) and (10).
Step 3: Compute the vectors $\Phi_t^{\eta}(t)$ from (12) and $\Phi_x(x)$, $\Phi_{xx}(x)$ from Equations (14) and (15).
Step 4: Compute the collocation points x_p and t_q.
Step 5: Compute the collocation points $s_{r,p}$ and $\mathtt{w}_r$.
Step 10: Solve the nonlinear system (21)–(24) and obtain the unknown vector $\mathbf{C}$.
Step 12.4: Let $u_{n,m}(x,t) = \Phi(x)^{\mathrm{T}} \mathbf{C} \Phi_t^{\eta}(t) + u_0(x)$.
Step 13: Post-processing the results.
Output: The approximate solution: $u(x,t) \simeq u_{n,m}(x,t)$.

4. Convergence Analysis

To further explore the behavior of the obtained numerical solution, this section presents a discussion of how the numerical solution $u_{n,m}(x,t)$ converges towards the exact solution $u(x,t)$.

Theorem 2. *Let $u_{n,m}(x,t)$ be the approximate solution of (1), $u(x,t)$ be its exact solution and $\mathscr{R}_{n,m}(x,t)$ be the residual error. Then,*

$$\sup_{(x,t)\in\Omega_{\mathtt{L}}\times\Omega_{\mathtt{T}}} |\mathscr{R}_{n,m}(x,t)| \leq \hat{\rho} \frac{n^3 + n + m + 1}{2^{n+m-8}},$$

where $\hat{\rho}$ is a positive constant.

Proof. Since $u_{n,m}(x,t)$ is the numerical solution of (1), thus

$$\begin{aligned} {}_0\mathscr{D}_t^{\eta} u_{n,m}(x,t) &= \mu \Delta u_{n,m}(x,t) + \beta \nabla u_{n,m}(x,t) + \mathscr{F}(x,t,u_{n,m}(x,t)) \\ &\quad + \frac{\kappa}{\zeta} \int_0^t e^{-\frac{t-s}{\zeta}} \Delta u_{n,m}(x,\mathrm{s}) \mathrm{ds} + \mathscr{R}_{n,m}(x,t). \end{aligned} \tag{25}$$

With reference to Equations (1) and (25), we have

$$\begin{aligned} |\mathscr{R}_{n,m}(x,t)| &\leq |{}_0\mathscr{D}_t^{\eta} \mathbf{e}_{n,m}(x,t)| + |\mu||\Delta \mathbf{e}_{n,m}(x,t)| + |\beta||\nabla \mathbf{e}_{n,m}(x,t)| \\ &\quad + \Big| \mathscr{F}(x,t,u(x,t)) - \mathscr{F}(x,t,\mathscr{U}_{n,m}(x,t)) \Big| \\ &\quad + |\frac{\kappa}{\zeta}| \Big| \int_0^t e^{-\frac{t-s}{\zeta}} \Delta \mathbf{e}_{n,m}(x,s) \mathrm{ds} \Big| \end{aligned} \tag{26}$$

where $\mathbf{e}_{n,m}(x,t) := u(x,t) - u_{n,m}(x,t)$. Using (5) and Theorem 1, results

$$
\begin{aligned}
|{}_0\mathscr{D}_t^{\eta}\mathbf{e}_{n,m}(x,t)| &\leq \frac{1}{\Gamma(1-\eta)}\int_0^t |(t-s)^{-\eta}|\Big|\frac{\partial \mathbf{e}_{n,m}}{\partial s}(x,s)\Big|\mathrm{d}s \\
&\leq \frac{b_1}{\Gamma(1-\eta)}\int_0^t \sup_{(x,t)\in\Omega_{\mathrm{L}}\times\Omega_{\mathrm{T}}}\Big|\frac{\partial \mathbf{e}_{n,m}}{\partial t}(x,t)\Big|\mathrm{d}s \\
&\leq \hat{\lambda}\frac{m}{2^{n+m-2}},
\end{aligned} \tag{27}
$$

where $\hat{\lambda} = \frac{\sigma b_1 \mathtt{T}}{\Gamma(1-\eta)}$ and b_1 is a positive constant depended on η and $\mathtt{T}$. The function $\mathscr{F}$ fulfills the Lipschitz condition in terms of u, hence

$$
\Big|\mathscr{F}(x,t,u(x,t)) - \mathscr{F}(x,t,u_{n,m}(x,t))\Big| \leq \xi_{\mathrm{F}}|\mathbf{e}_{n,m}(x,t)|,
$$

where $\xi_{\mathrm{F}} > 0$. From Theorem 1

$$
\Big|\mathscr{F}(x,t,u(x,t)) - \mathscr{F}(x,t,u_{n,m}(x,t))\Big| < \frac{\hat{c}\,\xi_{\mathrm{F}}}{2^{n+m}}. \tag{28}
$$

Moreover,

$$
\begin{aligned}
\Big|\int_0^t e^{-\frac{t-s}{\zeta}}\Delta\mathbf{e}_{n,m}(x,s)\mathrm{d}s\Big| &\leq \int_0^t \Big|e^{-\frac{t-s}{\zeta}}\Big||\Delta\mathbf{e}_{n,m}(x,s)|\mathrm{d}s \\
&\leq b_2\int_0^t \sup_{(x,t)\in\Omega_{\mathrm{L}}\times\Omega_{\mathrm{T}}}|\Delta\mathbf{e}_{n,m}(x,s)|\mathrm{d}s \\
&\leq b_2\mathtt{T}\hat{\sigma}\frac{n^3}{2^{n+m-8}},
\end{aligned} \tag{29}
$$

where b_2 is a positive constant depended on $\mathtt{T}$. Thus, from relations (26)–(29) and Theorem 1, we obtain

$$
\begin{aligned}
|\mathscr{R}_{n,m}(x,t)| &\leq \frac{\hat{\lambda}m + |\beta|\sigma n}{2^{n+m-2}} + (|\mu|\hat{\sigma} + |\frac{\kappa}{\zeta}|b_2\mathtt{T}\hat{\sigma})\frac{n^3}{2^{n+m-8}} + \frac{\hat{c}\,\xi_{\mathrm{F}}}{2^{n+m}} \\
&\leq \frac{\hat{\lambda}m + |\beta|\sigma n}{2^{n+m-8}} + (|\mu|\hat{\sigma} + |\frac{\kappa}{\zeta}|b_2\mathtt{T}\hat{\sigma})\frac{n^3}{2^{n+m-8}} + \frac{\hat{c}\,\xi_{\mathrm{F}}}{2^{n+m-8}} \\
&\leq \hat{\rho}\frac{n^3+n+m+1}{2^{n+m-8}},
\end{aligned}
$$

in which $\hat{\rho} = \max\{\hat{\lambda}, |\beta|\sigma, |\mu|\hat{\sigma} + |\frac{\kappa}{\zeta}|b_2\mathtt{T}\hat{\sigma}, \hat{c}\,\xi_{\mathrm{F}}\}$. As a result

$$
\sup_{(x,t)\in\Omega_{\mathrm{L}}\times\Omega_{\mathrm{T}}}|\mathscr{R}_{n,m}(x,t)| \leq \hat{\rho}\frac{n^3+n+m+1}{2^{n+m-8}}.
$$

□

5. Numerical Example

Herein, we implement the described method for solving some numerical examples to investigate the applicability and practical computational efficiency. To assess the accuracy of the scheme, let $n = m$, and the l_∞-norm error be given as

$$
\|\mathscr{E}^n\|_\infty = \max_{(\nu_p,\tau_q)}\Big|u(\nu_p,\tau_q) - u_n(\nu_p,\tau_q)\Big|, \tag{30}
$$

where $u_n(\nu_p,\tau_q)$ is an approximate solution of $u(x,t)$ at the designated collocation nodes $x = \nu_p$, $t = \tau_q$ and $p,q = 1,\ldots,n$. In which case, convergence order (CO) with respect to the l_∞-norm is as given by

$$\mathtt{CO} = \log_{\frac{n_1}{n_2}} \frac{\|\mathscr{E}^{n_1}\|_\infty}{\|\mathscr{E}^{n_2}\|_\infty}. \tag{31}$$

For numerical computations, a personal computer with a 1.70 GHz processor was used. In addition the computational software of choice was MatLab.

Example 1. *Solve the following FFKPPE*

$${}_0\mathscr{D}_t^{\eta} u(x,t) = u_{xx}(x,t) - u_x(x,t) + \sin(u(x,t)) + \frac{1}{5}\int_0^t e^{-\frac{t-s}{5}} u_{xx}(x,\mathrm{s})\mathrm{ds} + f(x,t),$$

with $\Omega_{\mathtt{L}} = \Omega_{\mathtt{T}} = [0,1]$ *and*

$$\begin{aligned} u(x,0) &= 0, && x \in \Omega_{\mathtt{L}}, \\ u^2(0,t) &= u(\mathtt{L},t) = 0, && t \in \Omega_{\mathtt{T}}. \end{aligned}$$

Here, the problem's exact solution is

$$u(x,t) = 10t^2x^3(1-x).$$

Figure 1 displays the exact (a) and numerical (b) solutions of $u(x,t)$ for $\eta = 0.75$, $\mathtt{M} = 5$ and $n = 8$. Where as, Figure 2 shows the absolute error and their respective contour plots for $u(x,t)$ given by $n = 8$ and $n = 10$ when $\eta = 0.5$ and $\mathtt{M} = 7$. In addition, Table 1 presents convergence results for the numerical solution of $u(x,t)$. These include the convergence order, l_∞-norm errors and CPU-time (sec.) for different values of n when $\mathtt{M} = 7$.

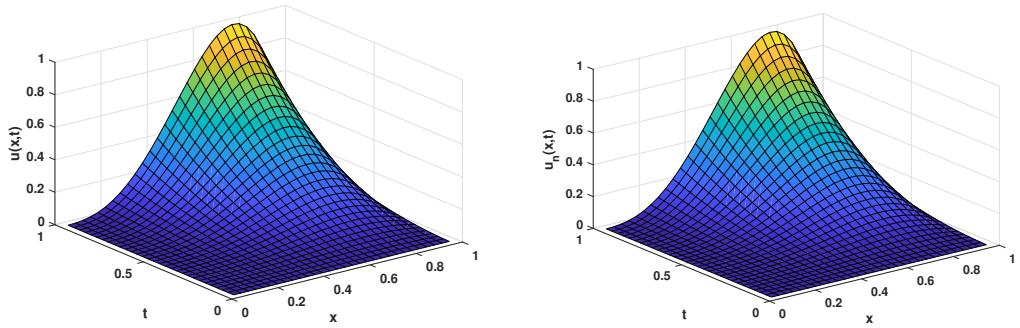

(**a**) (**b**)

Figure 1. A diagrammatic comparison of the exact and numerical solutions for Example 1 with $\eta = 0.75$. (**a**) Exact solution; (**b**) Numerical solution.

Table 1. Convergence analysis results for different values of n for Example 1.

	$\eta = 0.25$		$\eta = 0.75$		
n	$\|\mathscr{E}^n\|_\infty$	CO	$\|\mathscr{E}^n\|_\infty$	CO	CPU-Time
3	4.0670×10^{-2}	–	3.6422×10^{-2}	–	2.277
6	1.6720×10^{-3}	4.6042	5.4643×10^{-4}	6.0586	7.534
9	4.0740×10^{-5}	9.1613	1.0513×10^{-5}	9.7436	33.884
12	5.0991×10^{-7}	15.2277	1.1055×10^{-07}	15.8333	76.46

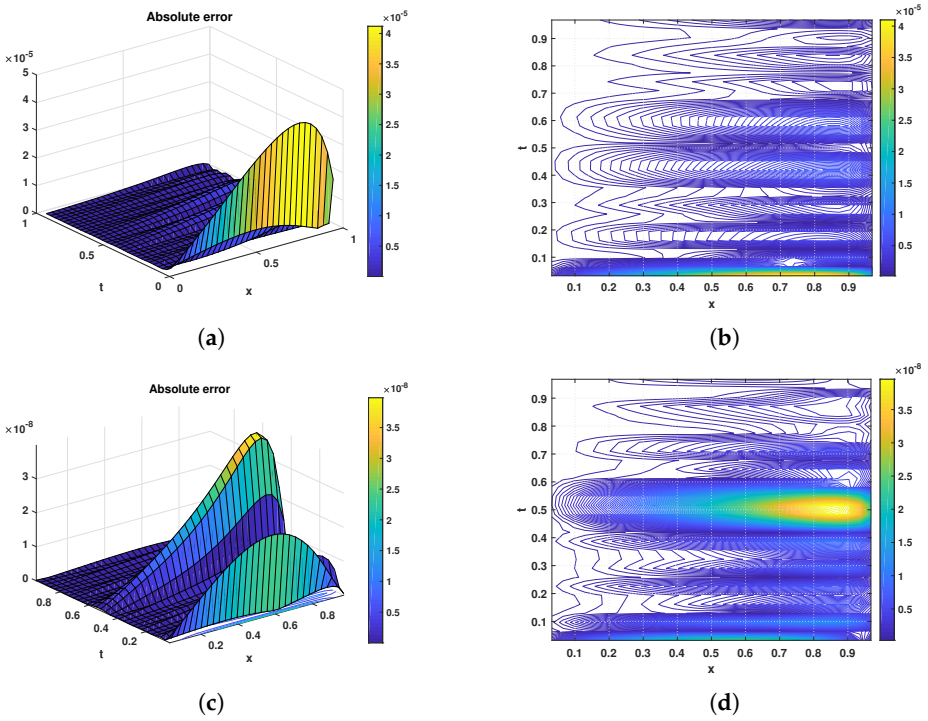

(**a**) (**b**)

(**c**) (**d**)

Figure 2. Plots indicating absolute errors and error contours for $u(x,t)$, given $n = 8$ and $n = 10$, with $\eta = 0.5$ in the domain Ω for Example 1. (**a**) Absolute error with $n = 8$; (**b**) Error contour with $n = 8$; (**c**) Absolute error with $n = 10$; (**d**) Error contour with $n = 10$.

Example 2. *Solve the following FFKPPE*

$$ {}_0D_t^{\eta} u(x,t) = -u_{xx}(x,t) + u^2(x,t) + \int_0^t e^{-(t-s)} u_{xx}(x,\mathrm{s})\mathrm{ds} + f(x,t), $$

where $\Omega_{\mathrm{L}} = \Omega_{\mathrm{T}} = [0,1]$ *and*

$$ \begin{aligned} u(x,0) &= 0, & x &\in \Omega_L, \\ u(0,t) &= 0, & x &\in \Omega_T, \\ -u(1,t) + u_x(1,t) &= 2\pi t, & t &\in \Omega_T. \end{aligned} $$

Here, the problem's exact solution is given by

$$ u(x,t) = tx\sin(2\pi x). $$

Figure 3 displays plots for the exact (a) and numerical (b) solutions of $u(x,t)$ when $\eta = 0.5$, $\mathtt{M} = 5$ and $n = 8$. Whereas the Figure 4 shows plots for the absolute errors and their respective contour plots for $u(x,t)$ given $n = 4$ and $n = 8$, when $\eta = 0.65$ and $\mathtt{M} = 7$. In addition, Table 2 presents convergence results for the numerical solution of $u(x,t)$. These include l_∞-norm errors, the convergence order as well as CPU run time in seconds (s) for different values of n when $\mathtt{M} = 6$.

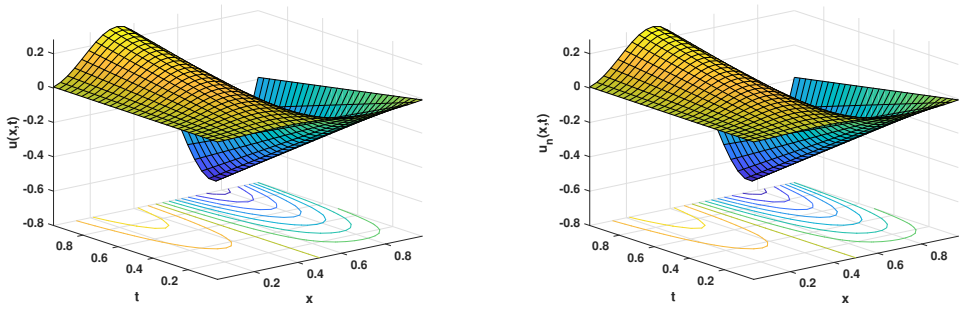

(**a**) (**b**)

Figure 3. A diagrammatic comparison of the exact and numerical solutions for Example 2 with $\eta = 0.5$. (**a**) Exact solution; (**b**) Numerical solution.

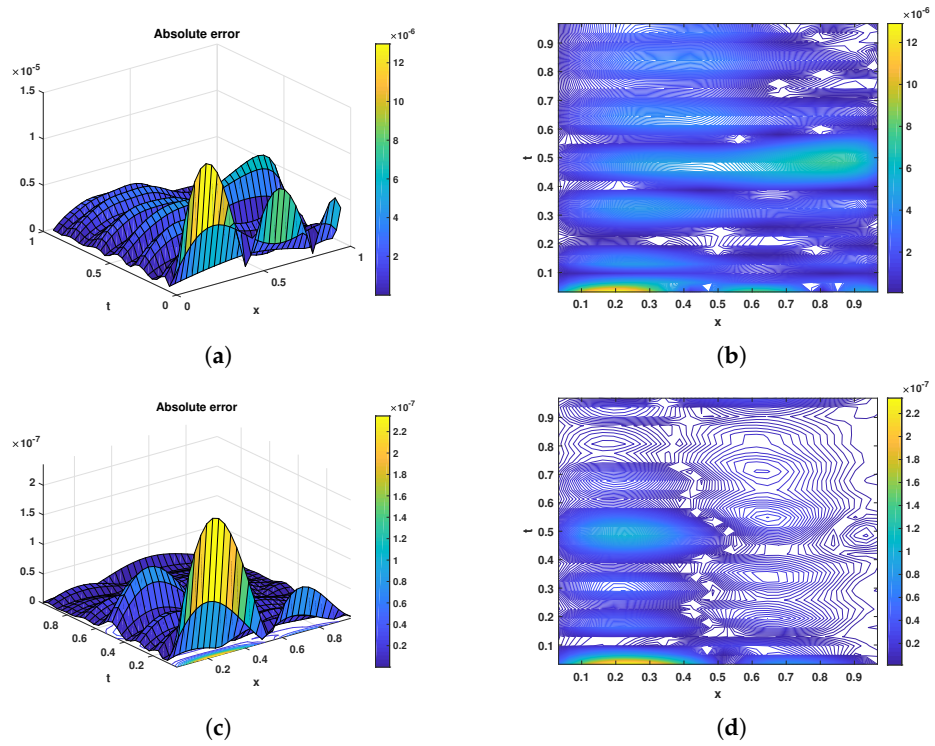

(**a**) (**b**)

(**c**) (**d**)

Figure 4. Plots indicating absolute errors and error contours for $u(x,t)$ with $n = 12$ and $n = 15$ when $\eta = 0.65$ in Ω for Example 2. (**a**) Absolute error with $n = 12$; (**b**) Error contour with $n = 12$; (**c**) Absolute error with $n = 15$; (**d**) Error contour with $n = 15$.

Table 2. Convergence analysis results for different values of n for Example 2.

	$\eta = 0.25$		$\eta = 0.75$		
n	$\|E^n\|_\infty$	CO	$\|E^n\|_\infty$	CO	CPU-Time
3	6.3855×10^{-1}	–	3.7469×10^{-1}	–	2.34
6	3.4551×10^{-2}	4.2080	8.2972×10^{-2}	5.4969	4.215
9	2.5097×10^{-3}	6.4673	1.8042×10^{-4}	9.4419	15.116
12	7.2113×10^{-5}	12.3389	5.2019×10^{-6}	12.3271	70.638

Example 3. *Solve the following generalized Fisher–Kolmogorov–Petrovskii–Piskunov [17]*

$$u_t(x,t) = -\frac{1}{2\pi^2}u_{xx}(x,t) + u^2(x,t) + \int_0^t e^{-\frac{(t-s)}{2}}u_{xx}(x,s)\mathrm{d}s + f(x,t),$$

where $(x,t) \in (0,1) \times (0,1]$ *and*

$$\begin{aligned} u(x,0) &= \sin(\pi x), & x &\in [0,1], \\ u(0,t) + u_x(0,t) &= \pi e^{-t/2}, & t &\in (0,1], \\ u(1,t) + u_x(1,t) &= -\pi e^{-t/2}, & t &\in (0,1]. \end{aligned}$$

Here, the problem's exact solution is given by

$$u(x,t) = e^{-t/2} \sin(\pi x).$$

Figure 5 displays plots for the exact (a) and numerical (b) solutions of $u(x,t)$ when $\mathtt{M} = 7$ and $n = 12$. Figure 6 shows plots for the absolute error and contour plot for $u(x,t)$, when $n = 12$ and $\mathtt{M} = 7$.

Table 3 shows the relative errors of the results obtained by the proposed method in comparison with the results of the spline collocation method [17], at time-level $t = 1.0$ for different values of n and $\mathtt{M} = 8$.

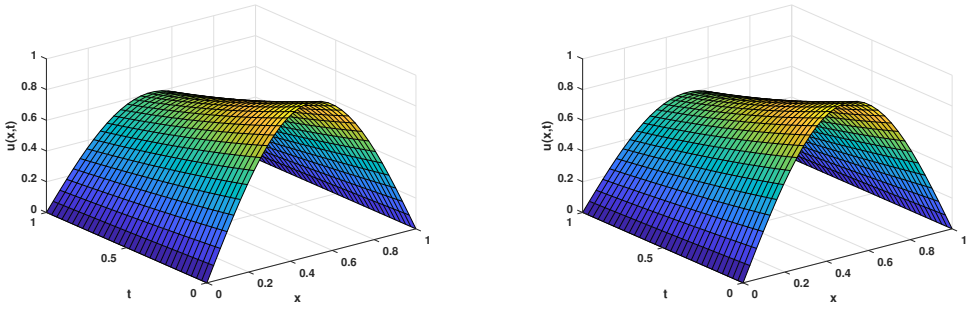

(**a**) (**b**)

Figure 5. A diagrammatic comparison of the exact and numerical solutions for Example 3 with $n = 12$. (**a**) Exact solution; (**b**) Numerical solution.

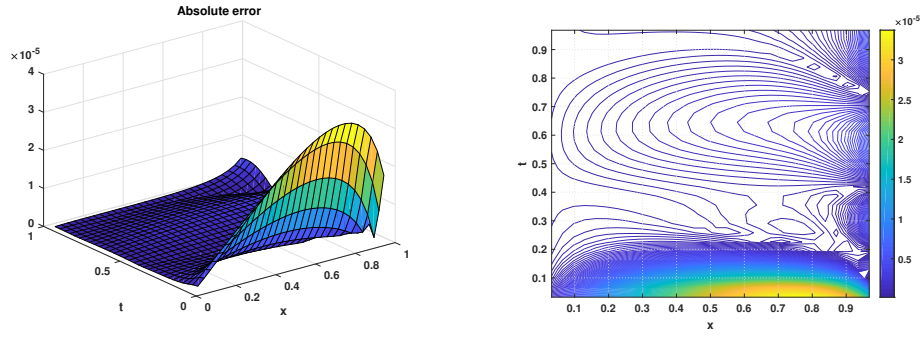

(**a**) (**b**)

Figure 6. Plots indicating absolute errors and error contours for $u(x,t)$ with $n = 12$ for Example 3. (**a**) Absolute error; (**b**) Error contour.

Table 3. Maximum absolute errors at time-level $t = 1.0$ for different values of n for Example 3.

B-Spline Method [17]		**Proposed Method**		
n	**Max | Error |**	n	$\|\|E^n\|\|_\infty$	CPU-Time
20	1.3×10^{-2}	3	2.4155×10^{-1}	2.124
30	7.4×10^{-3}	6	3.0031×10^{-3}	5.461
40	5.4×10^{-3}	9	2.2521×10^{-4}	17.36
50	4.4×10^{-3}	12	2.4747×10^{-6}	66.871

6. Conclusions

Shifted Chebyshev polynomials of the sixth-kind form the backbone of the numerical scheme that we have discussed in this research. Through these polynomials, we were able to construct a differential matrix and write an equation that approximates the solution of a differential equation with fractional order. The role of the collocation technique in our solution procedure is to augment the number of equations created from the initial and boundary conditions. Graphical comparisons of the results attained from this numerical scheme and the known exact solutions indicate that this scheme has a high level of accuracy. We also note that, as we increase the number of polynomials used, the accuracy and convergence rates also improve although this is accompanied by more intensive labor. Fortunately, it is clear from the results that we need a few polynomials to reach accepted level of accuracy.

Author Contributions: Conceptualization, methodology and software, S.B. and D.Z.; formal analysis, A.B.; investigation, J.A. and S.P.M.; writing—original draft preparation, D.Z., A.B. and S.B.; writing—review and editing, H.J., J.A. and S.P.M.; supervision, A.B., S.B. and H.J. All authors have read and agreed to the published version of the manuscript.

Funding: This research received no external funding.

Acknowledgments: Jehad Alzabut is thankful to Prince Sultan University and OSTİM Technical University for their endless support.

Conflicts of Interest: The authors declare no conflict of interest.

References

1. Baeumer, B.; Benson, D.Z.; Meerschaert, M.M.; Wheatcraft, S.W. Subordinated advection-dispersion equation for contaminant transport. *Water Resour. Res.* **2001**, *37*, 1543–1550. [CrossRef]
2. Mainardi, F.; Raberto, M.; Gorenelo, R.; Scalas, E. Fractional calculus and continuous-time finance II: The waiting-time discribution. *Phys. A Stat. Mech. Its Appl.* **2000**, *287*, 468–481. [CrossRef]
3. Javidi, M.; Ahmad, B. Numerical solution of fractional partial differential equations by numerical Laplace inversion technique. *Adv. Differ. Equ.* **2013**, *2013*, 375. [CrossRef]
4. Oldham, K.; Spanier, J. *The Fractional Calculus*; Academic Press: New York, NY, USA, 1974.
5. Srivastava, H.M. Some parametric and argument variations of the operators of fractional calculus and related special functions and integral transformations. *J. Nonlinear Convex Anal.* **2021**, *22*, 1501–1520.
6. Hosseini, V.R.; Shivanian, E.; Chen, W. Local integration of 2-D fractional telegraph equation via local radial point interpolant approximation. *Eur. Phys. J. Plus* **2015**, *130*, 1–21. [CrossRef]
7. Esmaeelzade Aghdam, Y.; Safdari, H.; Azari, Y.; Jafari, H.; Baleanu, D. Numerical investigation of space fractional order diffusion equation by the Chebyshev collocation method of the fourth kind and compact finite difference scheme. *Discret. Contin. Dyn. Syst.-S* **2021**, *14*, 2025–2039.
8. Ali, I.; Haq, S.; Nisar, K.S.; Baleanu, D. An efficient numerical scheme based on Lucas polynomials for the study of multidimensional Burgers-type equations. *Adv. Differ. Equ.* **2021**, *1*, 1–24. [CrossRef]
9. Hosseini, V.R.; Yousefi, F.; Zou, W.N. The numerical solution of high dimensional variable-order time fractional diffusion equation via the singular boundary method. *J. Adv. Res.* **2020**, *32*, 73–84. [CrossRef]
10. Abdelkawy, M.A.; Amin, A.Z.; Babatin, M.M.; Alnahdi, A.S.; Zaky, M.A.; Hafez, R.M. Jacobi spectral collocation technique for time-fractional inverse heat equations. *Fractal Fract.* **2021**, *5*, 115.
11. Nikan, O.; Avazzadeh, Z.; Tenreiro Machado, J.A. Numerical investigation of fractional nonlinear sine-Gordon and Klein-Gordon models arising in relativistic quantum mechanics. *Eng. Anal. Bound. Elem.* **2020**, *120*, 223–237. [CrossRef]
12. Babaei, A.; Jafari, H.; Banihashemi, S. A Collocation Approach for Solving Time-Fractional Stochastic Heat Equation Driven by an Additive Noise. *Symmetry* **2020**, *12*, 904. [CrossRef]
13. Zhang, X.; Yao, L. Numerical approximation of time-dependent fractional convection-diffusion-wave equation by RBF-FD method. *Eng. Anal. Bound. Elem.* **2021**, *130*, 1–9. [CrossRef]
14. Qiao, H.; Cheng, A. A fast finite difference/RBF meshless approach for time fractional convection-diffusion equation with non-smooth solution. *Eng. Anal. Bound. Elem.* **2021**, *125*, 280–289. [CrossRef]
15. Zaky, M.A.; Abdelkawy, M.A.; Ezz-Eldien, S.S.; Doha, E.H. Pseudospectral methods for the Riesz space-fractional Schrödinger equation. In *Fractional-Order Modeling of Dynamic Systems with Applications in Optimization*; Signal Processing and Control; Academic Press: Cambridge, MA, USA, 2022; pp. 323–353.
16. Branco, J.R.; Ferreira, J.A.; de Oliveira, P. Numerical methods for the generalized Fisher-Kolomogrov-Petrovskii-Piskunov equation. *Appl. Numer. Math.* **2007**, *57*, 89–102. [CrossRef]

17. Khuri, S.A.; Sayfy, A. A numerical approach for solving an extended Fisher-Kolomogrov-Petrovskii-Piskunov equation. *J. Comput. Appl. Math.* **2010**, *233*, 2081–2089. [CrossRef]
18. Machado, J.A.; Babaei, A.; Moghaddam, B.P. Highly accurate scheme for the Cauchy problem of the generalized Burgers-Huxley equation. *Acta. Polytech. Hung.* **2016**, *13*, 183–195.
19. Veeresha, P.; Prakasha, D.G.; Baleanu, D. An efficient numerical technique for the nonlinear fractional Kolmogorov-Petrovskii-Piskunov equation. *Mathematics* **2019**, *7*, 265. [CrossRef]
20. Podlubny, I. Fractional-order systems and PI/sup/spl lambda//D/sup/spl mull-Controllers. *IEEE Trans. Autom. Control* **1999**, *44*, 208–214. [CrossRef]
21. Leclerc, Q.J.; Lindsay, J.A.; Knight, G.M. Mathematical modelling to study the horizontal transfer of antimicrobial resistance genes in bacteria: Current state of the field and recommendations. *J. R. Soc. Interface* **2019**, *16*, 20190260. [CrossRef] [PubMed]
22. Khater, M.M.; Attia, R.A.; Abdel-Aty, A.H.; Alharbi, W.; Lu, D. Abundant analytical and numerical solutions of the fractional microbiological densities model in bacteria cell as a result of diffusion mechanisms. *Chaos Solitons Fractals* **2020**, *136*, 109824. [CrossRef]
23. Araújo, A.; Branco, R.; Ferreira, J.A. On the stability of a class of splitting methods for integro-differential equations. *Appl. Numer. Math.* **2009**, *59*, 436–453. [CrossRef]
24. Araújo, A.; Ferreira, J.A.; de Oliveira, P. Qualitative solutions for reaction-diffusion equations with memory. *Appl. Anal.* **2005**, *84*, 1231–1246. [CrossRef]
25. Araújo, A.; Ferreira, J.A.; de Oliveira, P. The effect of memory terms in diffusion phenomena. *J. Comput. Math.* **2006**, *24*, 91–102.
26. Barbeiro, S.; Ferreira, J.A. Integro-differential models for percutaneous drug absortion. *Int. J. Comput. Math.* **2007**, *84*, 451–467. [CrossRef]
27. Babaei, A.; Jafari, H.; Banihashemi, S. Numerical solution of variable order fractional nonlinear quadratic integro-differential equations based on the sixth-kind Chebyshev collocation method. *J. Comput. Appl. Math.* **2020**, *377*, 112908. [CrossRef]
28. Abd-Elhameed, W.M.; Youssri, Y.H. Fifth-kind orthonormal Chebyshev polynomial solutions for fractional differential equations. *Comput. Appl. Math.* **2018**, *37*, 2897–2921. [CrossRef]
29. Abd-Elhameed, W.M.; Youssri, Y.H. Sixth-kind Chebyshev spectral approach for solving fractional differential equations. *Int. J. Nonlinear Sci. Numer. Simul.* **2019**, *20*, 191–203. [CrossRef]
30. Canuto, C.; Hussaini, M.Y.; Quarteroni, A.; Zang, T.A. *Spectral Methods in Fluid Dynamics*; Springer: New York, NY, USA, 1988.